



WP2 – Propagation of the Solar Wind from the Sun to L1: Make the AWSoM time accurate using hourly ingested (GONG) magnetograms

Bart van der Holst (1), I. Sokolov (1), M. Liemohn (1), T. Arber (2)

(1) University of Michigan, Ann Arbor MI, USA

(2) University of Warwick

The research leading to these results was partly funded by the European Union's Horizon 2020 research and innovation program under grant agreement No 637302 PROGRESS



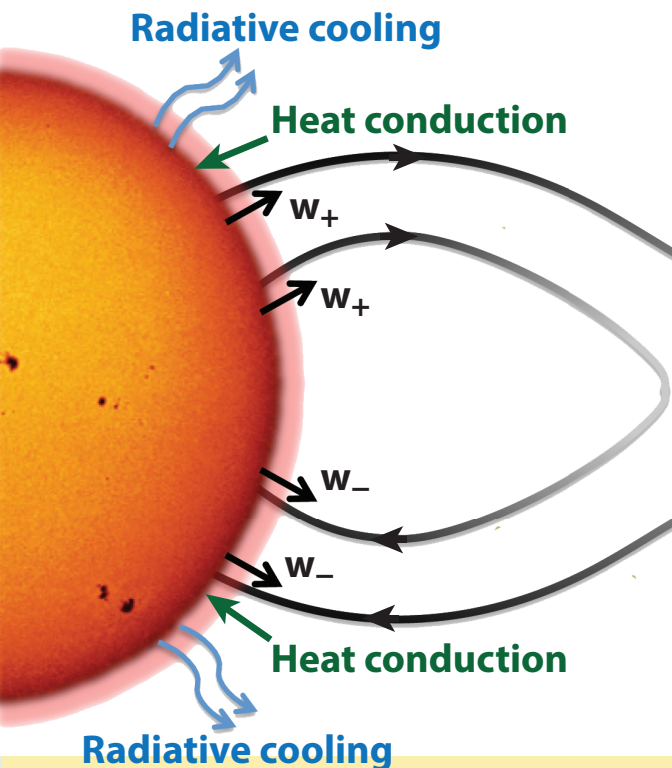
Alfvén Wave Solar Model (AWSoM)



I. Sokolov et al. ApJ **764**, 23 (2013)
 B. van der Holst et al. ApJ **782**, 81 (2014).

Extended MHD physics:

- Two (T_i, T_e) or three ($T_{i||}, T_{i\perp}, T_e$) temperatures
- Equations for parallel and antiparallel propagating turbulence (w_{\pm})
- Physics-based reflection of w_{\pm} results in turbulent cascade
- Physics-based apportioning of turbulence dissipation (at the gyro-radius scales) into coronal heating of various species
- Wave pressure gradient acceleration of solar wind plasma
- Collisional and collisionless electron heat conduction
- Radiative plasma cooling using CHIANTI



Boundary Conditions:

- Radial magnetic field is derived from synoptic solar magnetograms
- Poynting flux of outward propagating turbulence:

$$(S_A/B)_{\odot} = 1.1 \times 10^6 \text{ W m}^{-2} \text{ T}^{-1}$$

Alfvén Wave Turbulence



M Wave energy densities of counter-propagating transverse Alfvén waves parallel (+) and anti-parallel (-) to magnetic field:

energy reduction in expanding flow

wave dissipation

$$\frac{\partial w_{\pm}}{\partial t} + \nabla \cdot [(\mathbf{u} \pm \mathbf{V}_A)w_{\pm}] + \frac{w_{\pm}}{2}(\nabla \cdot \mathbf{u}) = \mp \mathcal{R}\sqrt{w_-w_+} - \Gamma_{\pm}w_{\pm}$$



Alfvén wave advection



wave reflection

$$\mathcal{R} = \min \left[\sqrt{(\mathbf{b} \cdot [\nabla \times \mathbf{u}])^2 + [(\mathbf{V}_A \cdot \nabla) \log V_A]^2}, \max(\Gamma_{\pm}) \right] \begin{cases} \left(1 - 2\sqrt{\frac{w_-}{w_+}}\right) & \text{if } 4w_- \leq w_+ \\ 0 & \text{if } 1/4w_- < w_+ < 4w_- \\ \left(2\sqrt{\frac{w_+}{w_-}} - 1\right) & \text{if } 4w_+ \leq w_- \end{cases}$$

M Phenomenological wave dissipation (Dmitruk et al., 2002): $\Gamma_{\pm} = \frac{2}{L_{\perp}} \sqrt{\frac{w_{\mp}}{\rho}}$

M Similar to Hollweg (1986), we use a simple scaling law for the transverse correlation length $L_{\perp} \sqrt{B} = 150 \text{ km } \sqrt{T}$

M Poynting flux of outward propagating turbulence:

$$(S_A/B)_{\odot} = 1.1 \times 10^6 \text{ W m}^{-2} \text{ T}^{-1}$$

- M Counter-propagating Alfvén waves due to partial reflection of the waves**
- M Non-linear interaction of these waves results in transverse energy cascade**
- M Wave dissipation at the gyro-kinetic scales**

- M We use the coronal heating formulation of Chandran et al. (2011):**
 - 🌍 Linear damping of kinetic Alfvén waves (KAW), resulting in **electron** and **parallel proton** heating
 - 🌍 Electric field fluctuations due to transverse turbulent cascade can disturb the proton gyro motion enough to give rise to perpendicular stochastic heating
 - 🌍 **Electron** heating at scales much smaller than proton gyro-radius

Limiting the Anisotropic Pressure

X. Meng et al. 2012 JCP, JGR

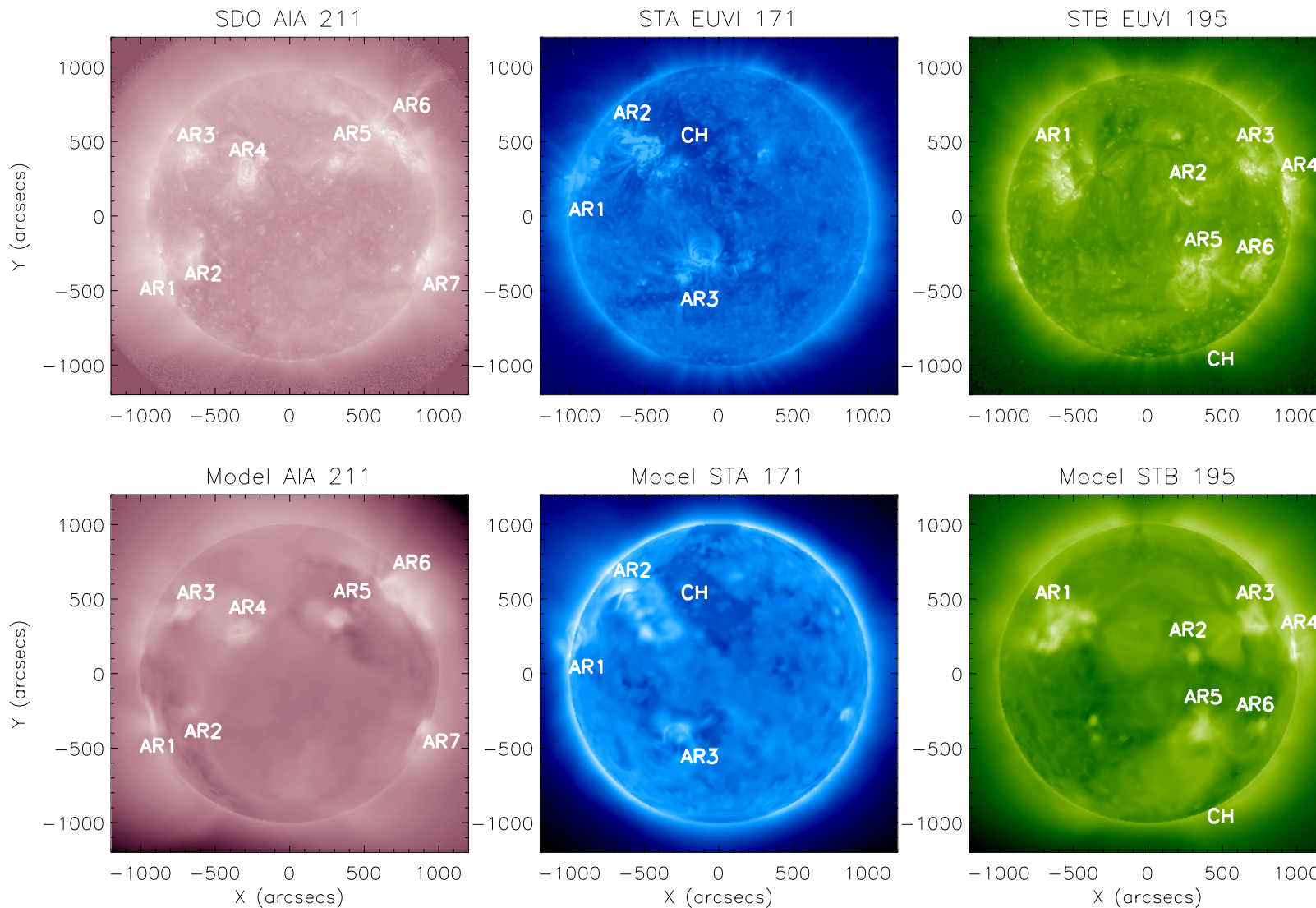
The instability-based anisotropic pressure relaxation towards the marginal stable pressure \bar{p}_{\parallel} while keeping averaged pressure p unmodified:

$$\frac{\delta p_{\parallel}}{\delta t} = \frac{\bar{p}_{\parallel} - p_{\parallel}}{\tau}$$

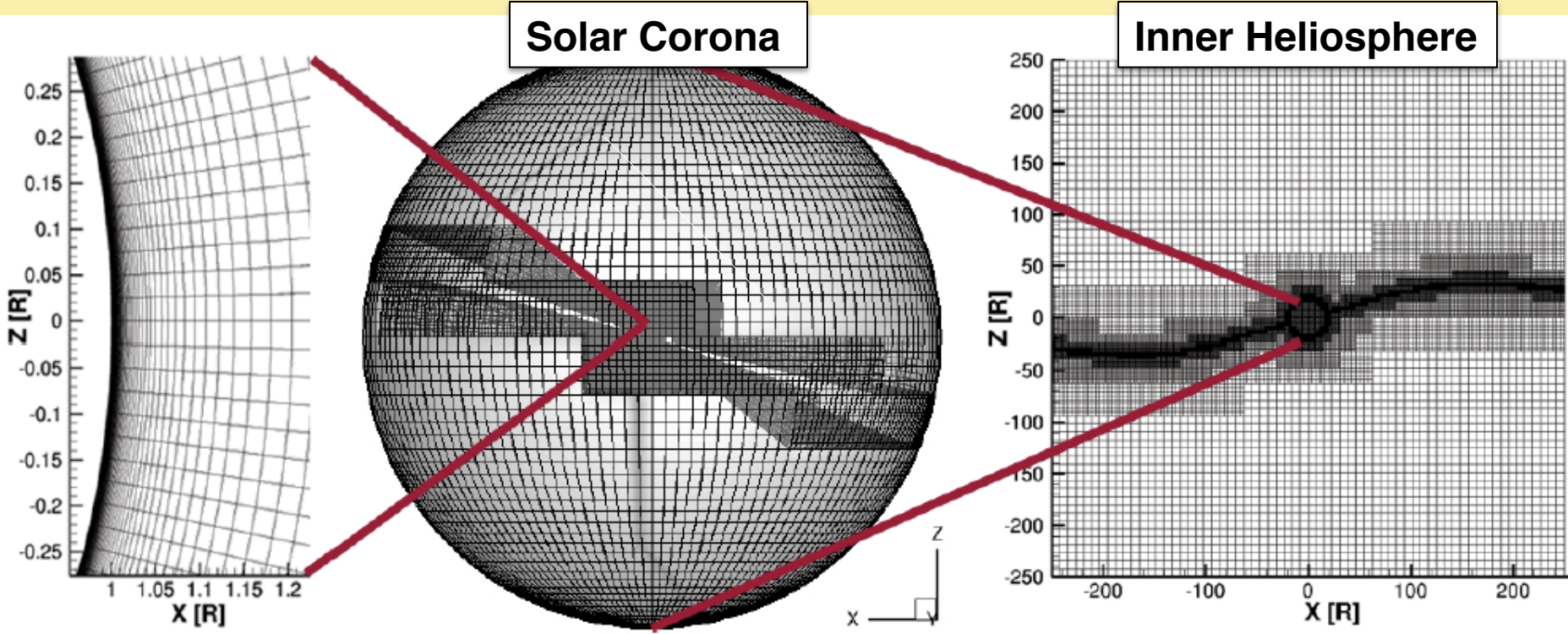
applied in firehose, mirror and proton cyclotron unstable regions. τ is taken to be the inverse of the growth rates of the instabilities (Hall 1979, 1980, 1981 and Southwood & Kivelson 1993):

	instability criteria	relaxation time τ
firehose	$\frac{p_{\parallel}}{p_{\perp}} > 1 + \frac{B^2}{\mu_0 p_{\perp}}$	$\tau_f = \frac{1}{\gamma_{f,max}} = \frac{2}{\Omega_i} \frac{\sqrt{p_{\parallel}(p_{\perp} - p_{\parallel}/4)}}{p_{\parallel} - p_{\perp} - B^2/\mu_0}$
mirror	$\frac{p_{\perp}}{p_{\parallel}} > 1 + \frac{B^2}{2\mu_0 p_{\perp}}$	$\tau_m = \frac{1}{\gamma_{m,max}} = \frac{3\sqrt{5}}{4\Omega_i} \sqrt{\frac{p_{\parallel}}{2(p_{\perp} - p_{\parallel}) - B^2 p_{\parallel}/(2\mu_0 p_{\perp})}}$
proton cyclotron	$\frac{p_{\perp}}{p_{\parallel}} > 1 + 0.3\sqrt{\frac{B^2}{2\mu_0 p_{\parallel}}}$	$\tau_{ic} = \frac{10^2}{\Omega_i}$

Validation: EUV Images for CR2107

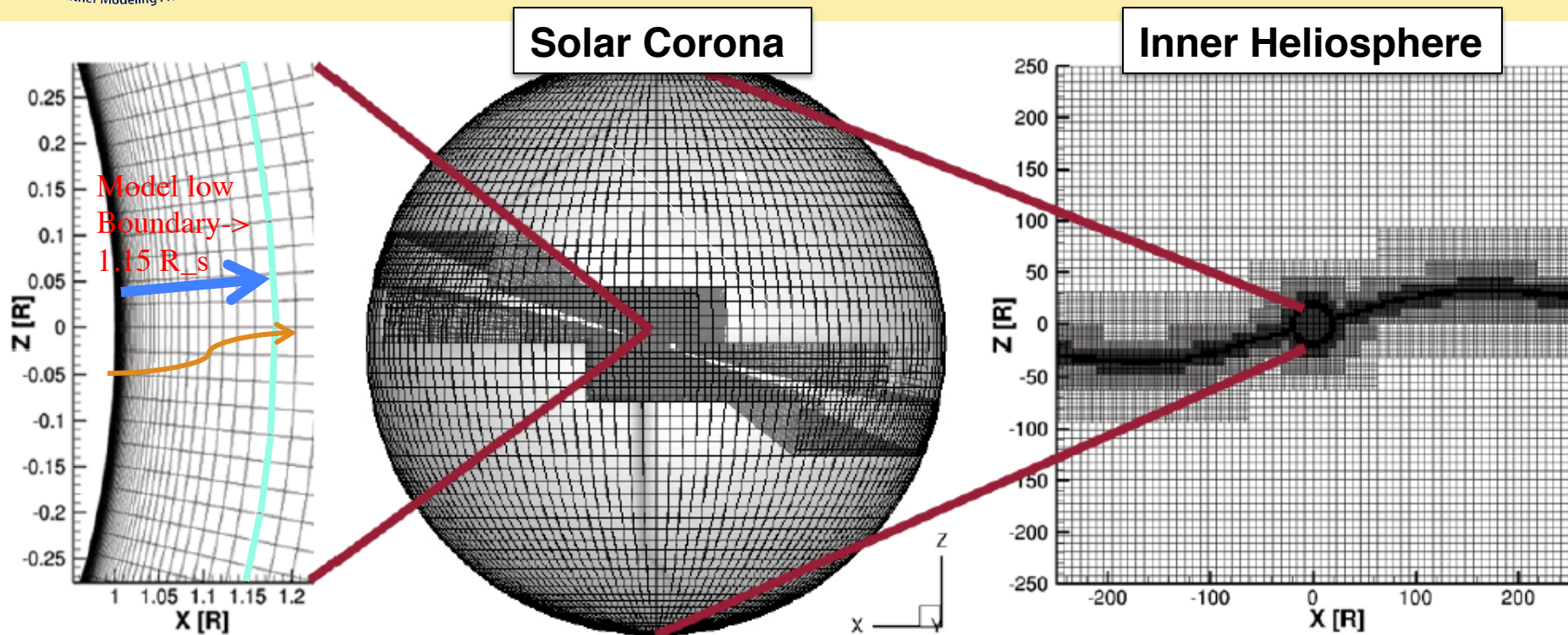


Computational Grid: AWSoM



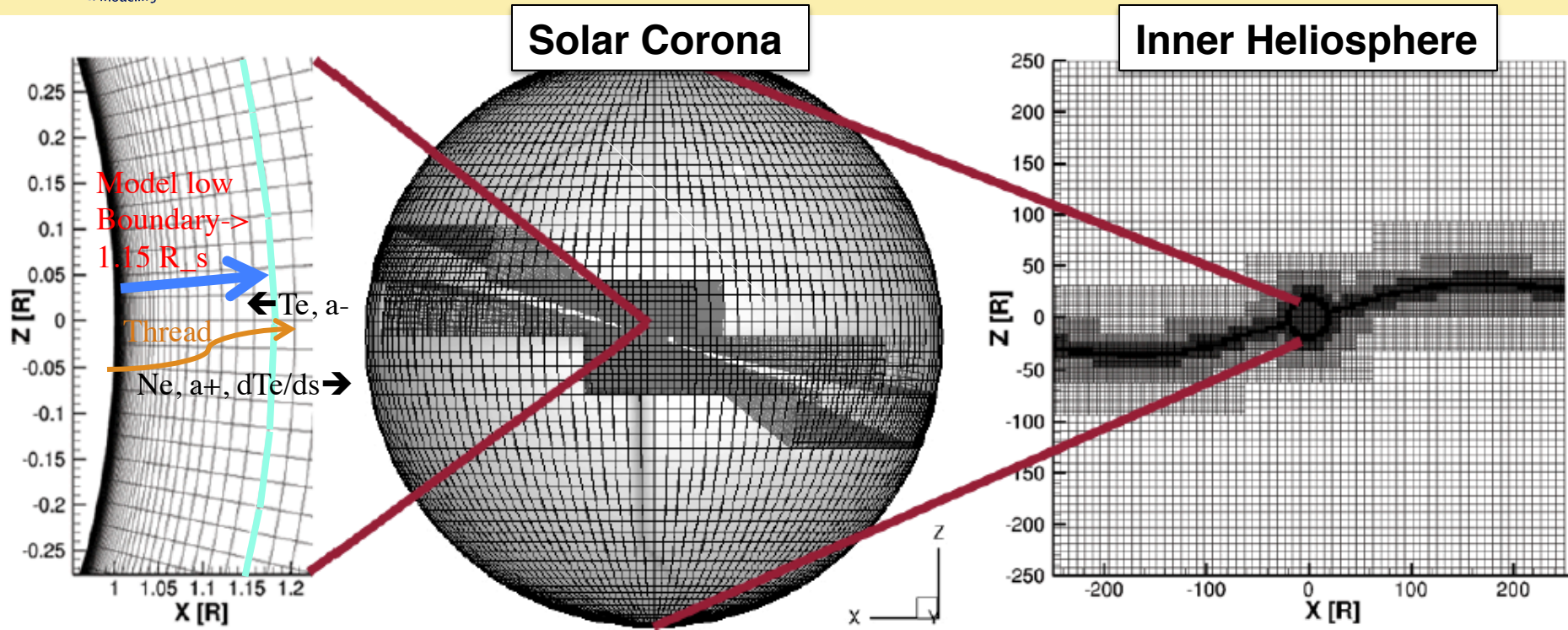
- M** AWSoM is split in two coupled framework components: stretched spherical grid for solar corona, cartesian grid for inner heliosphere
- M** Significant grid stretching to grid resolve the upper chromosphere and transition region in addition to artificial transition region broadening
- M** Due to the very high resolution below $1.15R_{\text{sun}}$ AWSoM is too slow to achieve faster than real-time.

AWSoM-R: Upshift the inner boundary



- M** We use the lower boundary of the model at $R = 1.15R_s$
- M** All resources spent to cover the low corona within the AWSoM model are saved in the AWSoM-R (significant speedup)

Apply 1D Thread Solution



- M** We apply 1D thread solutions along PFSS model field lines to bridge the ASoM-R model to the chromosphere through the transition region.
- M** Field-Line-Threaded approach allows us to both save computational resources and avoid severe limitation on the time step. Following the idea of the ‘radiation energy balance’ boundary condition (Lionello et al. 2009 and papers cited therein), we essentially extend its capability.

Threaded Field Line Model



M Recognize that between $1R_s$ and $1.15R_s$ $\mathbf{u} \parallel \mathbf{B}$ and $\mathbf{u} \ll \mathbf{V}_{\text{slow}}, \mathbf{V}_A, \mathbf{V}_{\text{fast}}$

M Inner boundary of AWSoM-R is at $1.15R_s$

M Each boundary cell center is connected to the upper chromosphere by a magnetic field line (of the PFSS model)

M Quasi-steady-state mass, momentum and energy transport is solved along the connecting field line (**1D** equations!)

$$\frac{\rho}{B} u_{\parallel} = \text{const} \quad \frac{d}{ds} \left[nk_B(T_e + T_i) + \frac{w_+ + w_-}{2} \right] = -\rho \frac{d}{ds} \left(\frac{GM_{\odot}}{r} \right)$$

$$B \frac{d}{ds} \left[\frac{\rho}{B} u_{\parallel} \left(\frac{5k_B(T_e + T_i)}{2m_p} - \frac{GM_{\odot}}{r} \right) + \frac{w_+ - w_-}{\sqrt{\mu_0 \rho}} - \frac{\kappa_0 T^{5/2}}{B} \frac{dT_e}{ds} \right] = -n^2 \Lambda(T_e)$$

$$\nabla \cdot [(\mathbf{u} \pm \mathbf{V}_A)w_{\pm}] + \frac{w_{\pm}}{2} (\nabla \cdot \mathbf{u}) = \mp \mathcal{R} \sqrt{w_- w_+} - \Gamma_{\pm} w_{\pm}$$

Wave Energy Transport in TFL Model



M Energy transport $\nabla \cdot [(\mathbf{u} \pm \mathbf{V}_A)w_{\pm}] + \frac{w_{\pm}}{2}(\nabla \cdot \mathbf{u}) = \mp \mathcal{R}\sqrt{w_-w_+} - \Gamma_{\pm}w_{\pm}$

M In the upper chromosphere (near lower boundary) $V_A \gg u$ and all terms containing u can be neglected

M Assuming that near the chromosphere the Poynting flux (S_A) to magnetic field ratio is constant we can introduce a new dimensionless variable (a_{\pm})

$$w_{\pm} = \frac{S_A}{B} \sqrt{\mu_0 \rho} a_{\pm}^2$$

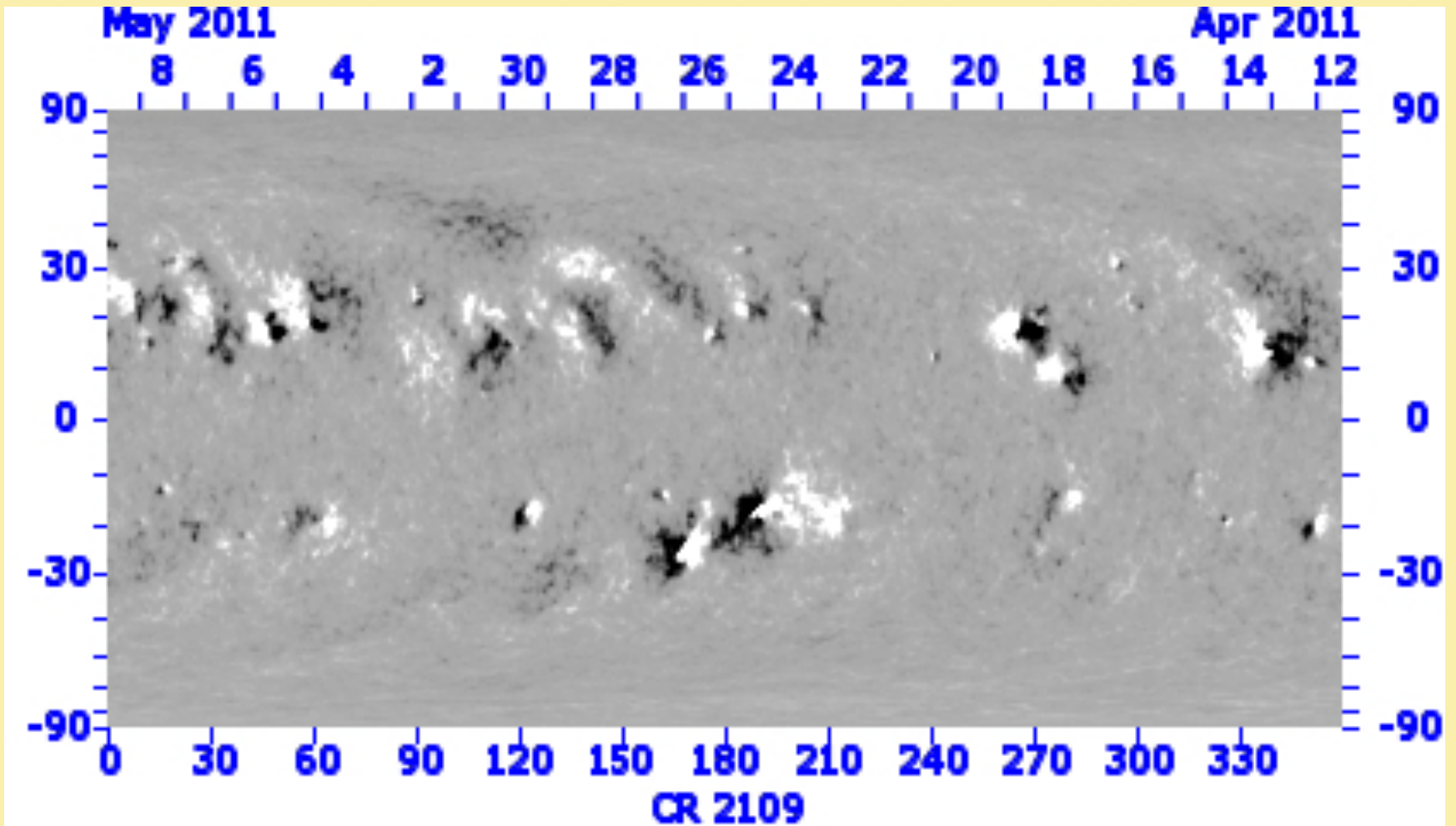
M Now the wave equation near the lower boundary is

$$\pm 2V_A \frac{da_{\pm}}{ds} = \mp \mathcal{R}a_{\mp} - \Gamma_{\pm}a_{\pm}$$

M Boundary condition at chromospheric boundary

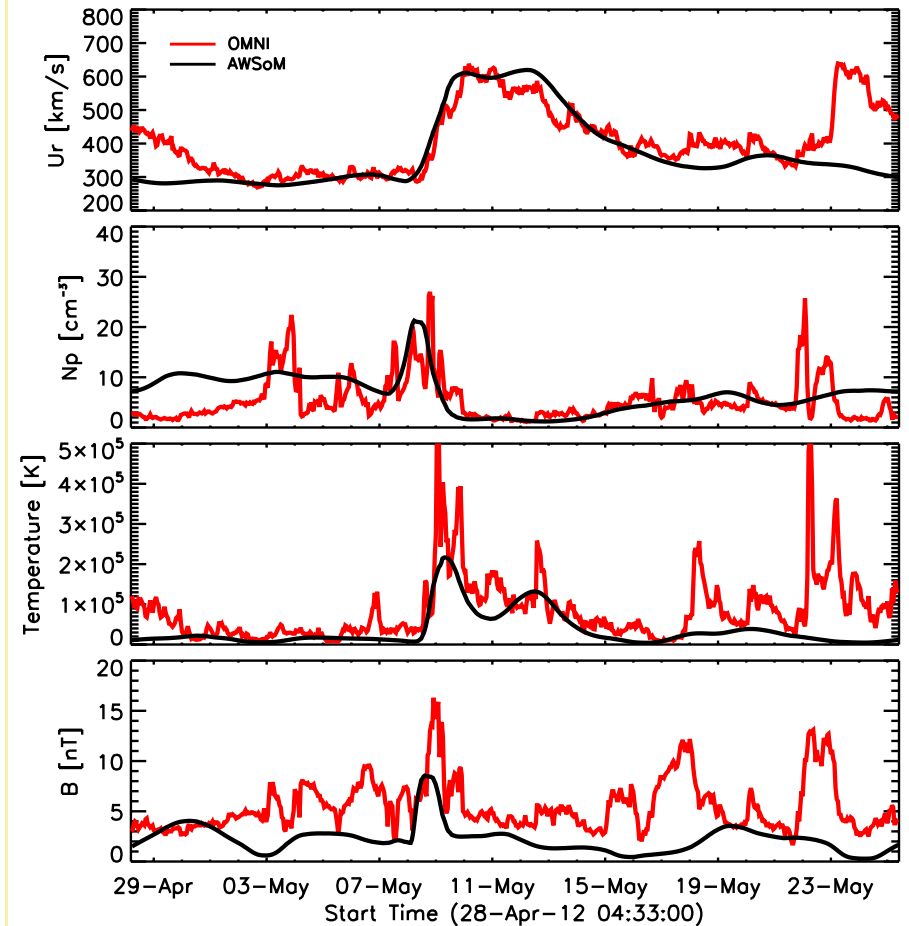
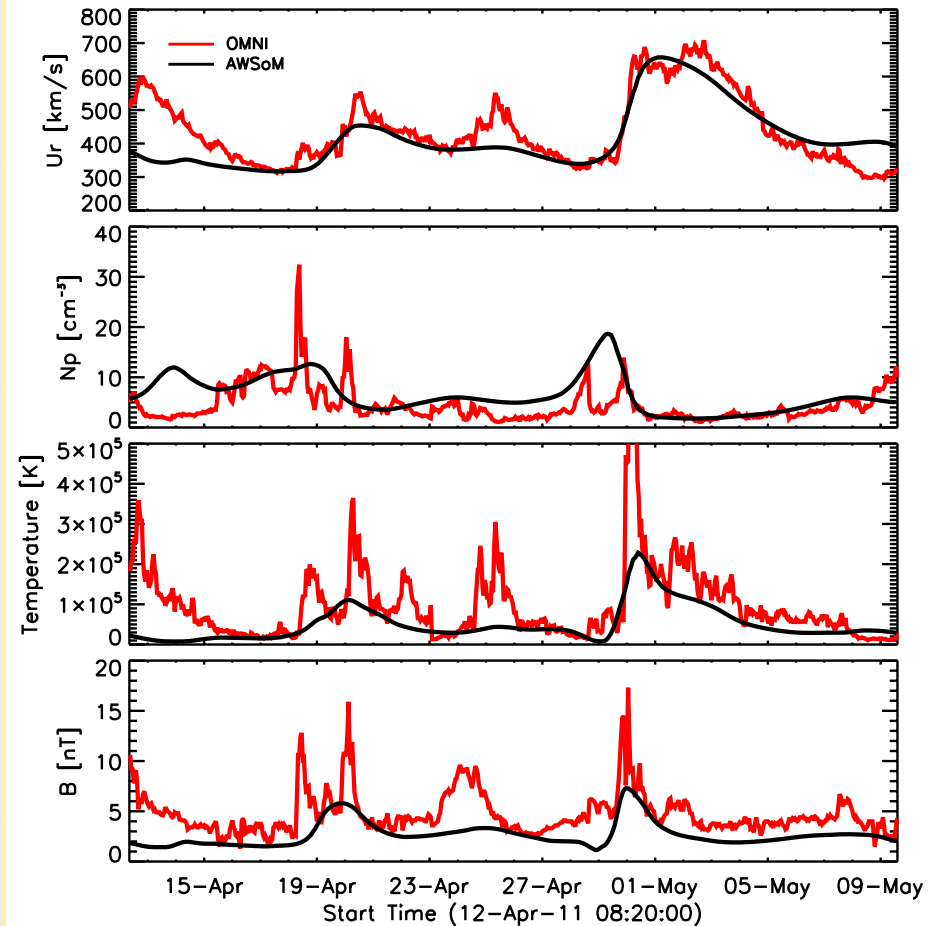
- Dimensionless amplitude is unity for outgoing wave
- Dimensionless amplitude has zero gradient for incoming wave

GONG Synoptic Magnetogram for CR2109



CR2109

CR2123



M Significant speed-up (about 200 times) of the 3D global solar corona and inner heliosphere model AWSoM:

- 1D solutions between $1 R_{\text{sun}}$ and $1.15 R_{\text{sun}}$ along PFSS model field lines provide inner boundary conditions at $1.15 R_{\text{sun}}$
- AWSoM real-time runs now require ~ 120 processor cores

M Future work involves:

- Couple corona part of AWSoM and inner heliosphere SWIFT
- Validate the AWSoM/SWIFT codes for historical magnetograms and WIND/ACE data
- Run real-time test of predicted L1 variables based on coupled AWSoM/SWIFT codes